

Refractive index and dispersion control of ultrafast laser inscribed waveguides in gallium lanthanum sulphide for near and mid-infrared applications

Giorgos Demetriou,¹ Jean-Philippe Bérubé,² Réal Vallée,² Younès Messaddeq,² Christian R. Petersen,³ Deepak Jain,³ Ole Bang,³ Chris Craig,⁴ Daniel W. Hewak,⁴ and Ajoy K Kar^{1,*}

¹*Institute of Photonics and Quantum Sciences, School of Engineering and Physical Sciences, David Brewster Building, Heriot-Watt University, Edinburgh, EH11 4AS, UK*

²*Centre d'Optique, Photonique et Laser (COPL), Université Laval, 2375 rue de la Terrasse, Québec (Québec) G1V0A6, Canada*

³*DTU Fotonik, Department of Photonics Engineering, Technical University of Denmark, DK-2800 Kgs. Lyngby, Denmark*

⁴*Optoelectronics Research Centre, University of Southampton, Southampton SO40 4UG, UK*
**a.k.kar@hw.ac.uk*

Abstract: The powerful ultrafast laser inscription technique is used to fabricate optical waveguides in gallium lanthanum sulphide substrates. For the first time the refractive index profile and the dispersion of such ultrafast laser inscribed waveguides are experimentally measured. In addition the Zero Dispersion Wavelength of both the waveguides and bulk substrate is experimentally determined. The Zero Dispersion Wavelength was determined to be between 3.66 and 3.71 μm for the waveguides and about 3.61 μm for the bulk. This work paves the way for realizing ultrafast laser inscribed waveguide devices in gallium lanthanum sulphide glasses for near and mid-IR applications.

©2016 Optical Society of America

OCIS codes: (160.4760) Optical properties; (160.2750) Glass and other amorphous materials.

References and links

1. R. E. Simpson, A. Mairaj, R. J. Curry, C.-C. Huang, K. Knight, N. Sessions, M. Hassan, and D. W. Hewak, "Electrical phase change of Ga:La:S:Cu films," *Electron. Lett.* **43**(15), 830–832 (2007).
2. Y. E. Romanyuk, H. Hagedorfer, P. Stücheli, P. Fuchs, A. R. Uhl, C. M. Sutter-Fella, M. Werner, S. Haass, J. Stückelberger, C. Broussillou, P.-P. Grand, V. Bermudez, and A. N. Tiwari, "All Solution-Processed Chalcogenide Solar Cells – from Single Functional Layers Towards a 13.8% Efficient CIGS Device," *Adv. Funct. Mater.* **25**(1), 12–27 (2015).
3. J. Hu, V. Tarasov, A. Agarwal, L. Kimerling, N. Carlie, L. Petit, and K. Richardson, "Fabrication and testing of planar chalcogenide waveguide integrated microfluidic sensor," *Opt. Express* **15**(5), 2307–2314 (2007).
4. B. J. Eggleton, B. Luther-Davies, and K. Richardson, "Chalcogenide photonics," *Nat. Photonics* **5**, 141–148 (2011).
5. J. R. Macdonald, R. R. Thomson, S. J. Beecher, N. D. Psaila, H. T. Bookey, and A. K. Kar, "Ultrafast laser inscription of near-infrared waveguides in polycrystalline ZnSe," *Opt. Lett.* **35**(23), 4036–4038 (2010).
6. J. Hodgkinson and R. P. Tatam, "Optical gas sensing: a review," *Meas. Sci. Technol.* **24**(1), 012004 (2013).
7. P. Lucas, M. A. Solis, D. L. Coq, C. Juncker, M. R. Riley, J. Collier, D. E. Boesewetter, C. Boussard-Plédel, and B. Bureau, "Infrared biosensors using hydrophobic chalcogenide fibers sensitized with live cells," *Sens. Actuators B Chem.* **119**(2), 355–362 (2006).
8. A. Ródenas, G. Martin, B. Arezki, N. Psaila, G. Jose, A. Jha, L. Labadie, P. Kern, A. Kar, and R. Thomson, "Three-dimensional mid-infrared photonic circuits in chalcogenide glass," *Opt. Lett.* **37**(3), 392–394 (2012).
9. J. McCarthy, H. Bookey, S. Beecher, R. Lamb, I. Elder, and A. K. Kar, "Spectrally tailored mid-infrared super-continuum generation in a buried waveguide spanning 1750 nm to 5000 nm for atmospheric transmission," *Appl. Phys. Lett.* **103**(15), 151103 (2013).

10. C. R. Petersen, U. Møller, I. Kubat, B. Zhou, S. Dupont, J. Ramsay, T. Benson, S. Sujecki, N. Abdel-Moneim, Z. Tang, D. Furniss, A. Seddon, and O. Bang, "Mid-infrared supercontinuum covering the 1.4–13.3 μm molecular fingerprint region using ultra-high NA chalcogenide step-index fibre," *Nat. Photonics* **8**(11), 830–834 (2014).
11. N. D. Psaila, R. R. Thomson, H. T. Bookey, S. Shen, N. Chiodo, R. Osellame, G. Cerullo, A. Jha, and A. K. Kar, "Supercontinuum generation in an ultrafast laser inscribed chalcogenide glass waveguide," *Opt. Express* **15**(24), 15776–15781 (2007).
12. J. E. McCarthy, H. T. Bookey, N. D. Psaila, R. R. Thomson, and A. K. Kar, "Mid-infrared spectral broadening in an ultrafast laser inscribed gallium lanthanum sulphide waveguide," *Opt. Express* **20**(2), 1545–1551 (2012).
13. T. Schweizer, D. Brady, and D. W. Hewak, "Fabrication and spectroscopy of erbium doped gallium lanthanum sulphide glass fibres for mid-infrared laser applications," *Opt. Express* **1**(4), 102–107 (1997).
14. G. Demetriou, F. Thorburn, A. Lancaster, C. Craig, E. Weatherby, D. W. Hewak, and A. Kar, "Fluorescence in Erbium Doped Gallium Lanthanum Sulphide: Potential for mid-IR Waveguide Laser," in *CLEO: 2015*, OSA 2015), STh1G.2.
15. J. R. Macdonald, S. J. Beecher, P. A. Berry, K. L. Schepler, and A. K. Kar, "Compact mid-infrared Cr:ZnSe channel waveguide laser," *Appl. Phys. Lett.* **102**(16), 161110 (2013).
16. A. Lancaster, G. Cook, S. A. McDaniel, J. Evans, P. A. Berry, J. D. Shephard, and A. K. Kar, "Mid-infrared laser emission from Fe:ZnSe cladding waveguides," *Appl. Phys. Lett.* **107**(3), 031108 (2015).
17. A. K. Mairaj, A. M. Chardon, D. P. Shepherd, and D. W. Hewak, "Laser performance and spectroscopic analysis of optically written channel waveguides in neodymium-doped gallium lanthanum sulphide glass," *IEEE J. Sel. Top. Quantum Electron.* **8**(6), 1381–1388 (2002).
18. J. A. Frantz, L. B. Shaw, J. S. Sanghera, and I. D. Aggarwal, "Waveguide amplifiers in sputtered films of Er³⁺-doped gallium lanthanum sulfide glass," *Opt. Express* **14**(5), 1797–1803 (2006).
19. K. S. Bindra, H. T. Bookey, A. K. Kar, B. S. Wherrett, X. Liu, and A. Jha, "Nonlinear optical properties of chalcogenide glasses: Observation of multiphoton absorption," *Appl. Phys. Lett.* **79**(13), 1939–1941 (2001).
20. M. Asobe, T. Kanamori, and K. Kubodera, "Ultrafast all-optical switching using highly nonlinear chalcogenide glass fiber," *IEEE Photonics Technol. Lett.* **4**(4), 362–365 (1992).
21. M. Asobe, T. Ohara, I. Yokohama, and T. Kaino, "Low power all-optical switching in a nonlinear optical loop mirror using chalcogenide glass fibre," *Electron. Lett.* **32**(15), 1396–1397 (1996).
22. T. D. Vo, H. Hu, M. Galili, E. Palushani, J. Xu, L. K. Oxenløwe, S. J. Madden, D. Y. Choi, D. A. P. Bulla, M. D. Pelusi, J. Schröder, B. Luther-Davies, and B. J. Eggleton, "Photonic chip based transmitter optimization and receiver demultiplexing of a 1.28 Tbit/s OTDM signal," *Opt. Express* **18**(16), 17252–17261 (2010).
23. M. D. Pelusi, V. G. Ta'eed, F. Libin, E. Magi, M. R. E. Lamont, S. Madden, C. Duk-Yong, D. A. P. Bulla, B. Luther-Davies, and B. J. Eggleton, "Applications of Highly-Nonlinear Chalcogenide Glass Devices Tailored for High-Speed All-Optical Signal Processing," *IEEE J. Sel. Top. Quantum Electron.* **14**(3), 529–539 (2008).
24. D. W. Hewak, R. C. Moore, T. Schweizer, J. Wang, B. Samson, W. S. Brocklesby, D. N. Payne, and E. J. Tarbox, "Gallium lanthanum sulphide optical fibre for active and passive applications," *Electron. Lett.* **32**(4), 384 (1996).
25. P. Bastock, C. Craig, K. Khan, E. Weatherby, J. Yao, and D. W. Hewak, "Properties of Gallium Lanthanum Sulphide Glass," in *CLEO: 2015*, OSA 2015), STh1G.1.
26. C. C. Huang, D. Hewak, and J. Badding, "Deposition and characterization of germanium sulphide glass planar waveguides," *Opt. Express* **12**(11), 2501–2506 (2004).
27. Z. G. Lian, W. Pan, D. Furniss, T. M. Benson, A. B. Seddon, T. Kohoutek, J. Orava, and T. Wagner, "Embossing of chalcogenide glasses: monomode rib optical waveguides in evaporated thin films," *Opt. Lett.* **34**(8), 1234–1236 (2009).
28. K. E. Youden, T. Grevatt, R. W. Eason, H. N. Rutt, R. S. Deol, and G. Wylangowski, "Pulsed laser deposition of Ga-La-S chalcogenide glass thin film optical waveguides," *Appl. Phys. Lett.* **63**(12), 1601–1603 (1993).
29. D. Choudhury, J. R. Macdonald, and A. K. Kar, "Ultrafast laser inscription: perspectives on future integrated applications," *Laser Photonics Rev.* **8**(6), 827–846 (2014).
30. K. M. Davis, K. Miura, N. Sugimoto, and K. Hirao, "Writing waveguides in glass with a femtosecond laser," *Opt. Lett.* **21**(21), 1729–1731 (1996).
31. R. R. Thomson, H. T. Bookey, N. D. Psaila, A. Fender, S. Campbell, W. N. Macpherson, J. S. Barton, D. T. Reid, and A. K. Kar, "Ultrafast-laser inscription of a three dimensional fan-out device for multicore fiber coupling applications," *Opt. Express* **15**(18), 11691–11697 (2007).
32. H. T. Bookey, R. R. Thomson, N. D. Psaila, A. K. Kar, N. Chiodo, R. Osellame, and G. Cerullo, "Femtosecond Laser Inscription of Low Insertion Loss Waveguides in Z-Cut Lithium Niobate," *IEEE Photonics Technol. Lett.* **19**(12), 892–894 (2007).
33. R. R. Thomson, T. A. Birks, S. G. Leon-Saval, A. K. Kar, and J. Bland-Hawthorn, "Ultrafast laser inscription of an integrated photonic lantern," *Opt. Express* **19**(6), 5698–5705 (2011).
34. Y. Nasu, M. Kohtoku, and Y. Hibino, "Low-loss waveguides written with a femtosecond laser for flexible interconnection in a planar light-wave circuit," *Opt. Lett.* **30**(7), 723–725 (2005).
35. R. Mary, D. Choudhury, and A. K. Kar, "Applications of Fiber Lasers for the Development of Compact Photonic Devices," *IEEE J. Sel. Top. Quantum Electron.* **20**(5), 72–84 (2014).
36. A. Roberts, E. Ampem-Lassen, A. Barty, K. A. Nugent, G. W. Baxter, N. M. Dragomir, and S. T. Huntington, "Refractive-index profiling of optical fibers with axial symmetry by use of quantitative phase microscopy," *Opt. Lett.* **27**(23), 2061–2063 (2002).

37. M. Kalal and K. A. Nugent, "Abel inversion using fast Fourier transforms," *Appl. Opt.* **27**(10), 1956–1959 (1988).
 38. C. W. Ponader, J. F. Schroeder, and A. M. Streltsov, "Origin of the refractive-index increase in laser-written waveguides in glasses," *J. Appl. Phys.* **103**(6), 063516 (2008).
 39. V. R. Bhardwaj, P. B. Corkum, D. M. Rayner, C. Hnatovsky, E. Simova, and R. S. Taylor, "Stress in femtosecond-laser-written waveguides in fused silica," *Opt. Lett.* **29**(12), 1312–1314 (2004).
 40. P. Hlubina, D. Ciprian, and M. Kadulová, "Measurement of chromatic dispersion of polarization modes in optical fibres using white-light spectral interferometry," *Meas. Sci. Technol.* **21**(4), 045302 (2010).
-

1. Introduction

Chalcogenide glasses (ChGs) are an important class of materials used in phase-change memories [1], solar cells [2], sensors [3] and photonics [4]. They contain as their main constituent one or more of the chalcogen elements S, Se and Te, covalently bonded to network formers such as As, Ge, Sb, Ga, Si or P [4,5]. The existence of a broad range of possible glass-forming systems with large composition space allows for glasses with optical properties which can be tailored and optimized for photonic applications. The particular nature of the covalent bonds in ChGs gives them unique properties for infrared, nonlinear and waveguide applications.

Recently the mid-IR region of the electromagnetic spectrum has been attracting a considerable amount of research interest due to the potential applications in gas sensors [6], biosensors [7] and stellar interferometry [8]. This growing interest creates the need for new host materials suitable for integrated optical devices that operate in mid-IR and ChGs are proving to be an excellent solution due to their excellent mid-IR transparency. ChGs provide high optical nonlinearities which coupled with their mid-IR transparency define them as excellent hosts for supercontinuum generation mid-IR sources for sensing applications [9–12]. Furthermore ChGs can be readily doped with rare earth elements. Their low phonon energies reduce multi-photon quenching, therefore giving rise to mid-IR transitions opening the potential for laser sources operating in this important wavelength region [13–18].

ChGs are particularly appealing candidates for telecommunication applications as well. The rapid development of optical communications requires novel materials with large and ultrafast nonlinear optical responses in the femtosecond or picosecond domain for fabricating compact and low-threshold all-optical switching (AOS) and processing devices. ChGs are a perfect match for such devices as they possess high nonlinear refractive index (up to ~500 times that of silica), low multi-photon absorption [19] and high photosensitivity, properties which allow for switching devices with shorter interaction lengths, lower switching threshold and higher figures of merit. The aforementioned properties combined with the strong confinement along with dispersion engineering achievable in fibre and waveguide devices makes ChGs a good platform for ultrafast nonlinear optics and also a key technology for future optical communications systems. Over the past years chalcogenide all-optical switching applications have been demonstrated [20,21], as well as other ultrafast optical nonlinear devices such as demultiplexers [22] and wavelength converters [23] proving the great potential of ChGs in all-optical networks (AON).

Out of all the ChGs gallium lanthanum sulphide (GLS) is a particularly attractive one and a much awaited alternative to toxic arsenic-based glasses. Presenting optical transparency from the visible extending in the infrared up to 10 μ m [24] and thermally stable up to 550°C [25]. In addition GLS can be melted in a large scale without the requirement of a sealed ampoule environment making production and processing safer, easier and more economical.

For many applications, optical circuits based on planar waveguides are often preferred over fibres. Attempts to fabricate chalcogenide waveguides in the past have included thermal evaporation combined with plasma etching [3], chemical vapour deposition [26], fine embossing [27] and direct pulsed laser deposition [28]. However for all these methods several stages of post-deposition annealing and processing are required. In this work we used the

ultrafast laser inscription (ULI) technique [29] to fabricate waveguides embedded in GLS substrates.

ULI is a powerful technique that relies on the nonlinear absorption of sub-bandgap photons to induce permanent structural changes to a material. These changes can manifest themselves in multiple ways including a change in refractive index [30]. This change of the refractive index enables the confinement and guiding of light in ULI waveguide structures in bulk substrates. The ULI process involves the use of ultrashort pulses of light tightly focussed within the volume of a dielectric material. The extremely high peak power of the ultrashort pulses generates extremely high intensities at the focal region causing the nonlinear light matter interaction on which ULI is based. As a consequence the induced modification can be localized at the high intensity region at the focus of the ultrashort pulse train. This gives ULI the distinct advantage of true three dimensional capabilities [31] over other waveguide fabrication techniques. Furthermore ULI is a single step rapid fabrication technique that does not require any post-processing and offers both geometric and material design freedom. ULI has been shown to be applicable on a multitude of materials including crystals [32], and amorphous semiconductors [12] and by using waveguide shaping techniques, mode sizes can be tailored for particular applications [33].

Due to the nature of the ULI technique, the particular geometrical distribution of the refractive index modification of the substrate at the focus of the ultrashort pulse train is difficult to control, which can have a large impact on the guiding properties of the fabricated devices. Therefore an evaluation of the refractive index profiles of the ULI fabricated waveguides will allow for a better understanding of the modification procedure and will also give valuable information about the nature of the nonlinear light matter interaction on which ULI is based. Most importantly the information gained regarding the effect the inscription parameters, such as waveguide cross-sections, inscription pulse energies and translation speeds, have upon refractive index profiles will provide extremely useful tools for tailoring the refractive index profiles of ULI fabricated structures for specific applications.

Another important consideration when designing ULI devices is the dispersion and its origin. The knowledge of the dispersion at the operating wavelength is essential and it is often desirable for optical devices to operate as close as possible to the Zero Dispersion Wavelength (ZDW). In this work, for the first time, the dispersion of both the bulk substrate and a series of ULI fabricated waveguides in GLS is measured over a wide region of the near and mid-IR spectrum from ~ 1.3 - $4.5 \mu\text{m}$. The dispersion measurements performed here allow for the determination of the ZDW of both the bulk and the ULI waveguides revealing that it lies in the mid-IR, thereby defining them as excellent candidates for devices that operate in that region. Furthermore a comparison between the dispersion of the bulk GLS and the ULI fabricated waveguides provides information about the origin of the waveguide dispersion and the effect the inscription parameters have upon it.

2. Waveguide fabrication

The waveguides were fabricated using a mode-locked Yb-doped fiber laser which emitted 360 fs pulses with a central wavelength of $1.045 \mu\text{m}$ and a pulse repetition rate of 500 kHz. The substrates were mounted on air bearing Aerotech stages and the pulses from the fabrication laser were focused inside the substrates to a depth of $240 \mu\text{m}$ from the top surface using 0.4 NA and 0.6 NA aspheric lenses. The pulse energies incident on the sample varied from 52 to 110 nJ using four different translation speeds, 1, 4, 8 and 12 mm/s with the substrates being moved perpendicular to the laser beam direction. The multi-scan inscription technique was used [34,35] yielding waveguides with rectangular cross-sections. After fabrication the input and output facets of the substrates were polished to optical quality. The optical quality of all the substrates used was very good; no variations in the waveguide properties were observed between different substrates, which points out one of the major advantages of the ULI technique. The guiding properties of the structures fabricated with this technique are easily

and accurately repeatable given that the quality of the substrates is ensured and the same inscription parameters are used.

3. Refractive index profiling

The quantitative phase microscopy (QPM) method [36] was used to obtain the refractive index profiles of the waveguides inscribed in the GLS glass substrate. The QPM commercial software (Iatia ltd.) proceeds from slightly defocused bright field images of the waveguide to extract a corresponding phase image. The refractive index profile is retrieved by applying an inverse Abel transform on this phase image [37]. Figure 1(a) shows the refractive index profiles of 5 different waveguides, fabricated in the same substrate, obtained with the method described above. The experimental error of this method is approximately 1 standard deviation of the averaged data [36].

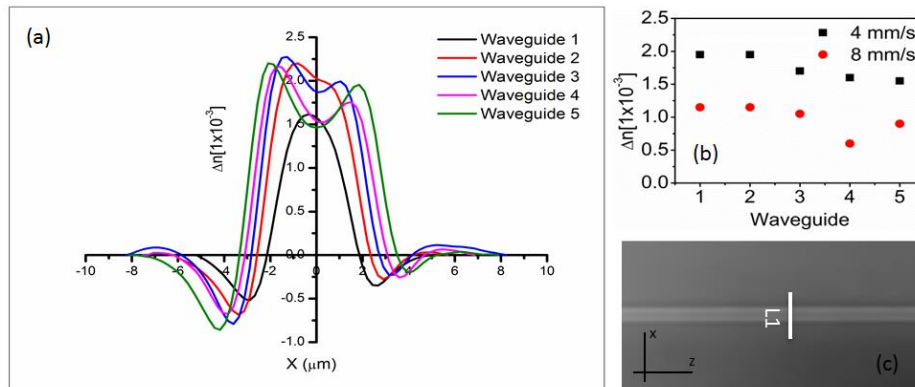


Fig. 1. (a) Refractive index profiles along the line L1 shown in (c) of 5 waveguides of different widths inscribed with pulse energy 72nJ and translation speed 12mm/s using a 0.6 NA aspheric lens. (b) Maximum Refractive index increase of two sets of waveguides (red and black) inscribed with different translation speeds using again a 0.6 NA aspheric lens and a pulse energy of 94 nJ. (c) Top view of a GLS waveguide with the line L1 along which the refractive index profile $\Delta n(x)$ is measured.

The waveguides were inscribed with a pulse energy of 72 nJ and a sample translation speed of 12mm/s using a 0.6 NA aspheric lens. Each waveguide was fabricated with different number of scans thus yielding waveguides of different sizes with waveguide 1 having the smallest cross-section and waveguide 5 having the biggest cross-section. Waveguide 1 was measured to have a width of about 4 μm and every subsequent waveguide was 0.66 μm wider than the previous one so that the widest waveguide had a width of about 6.6 μm . The height was the same for all waveguides, about 18 μm . The refractive index profile $\Delta n(x)$ measured along the line L1 for each of the waveguides is shown in Fig. 1(a).

Figure 1(b) shows the maximum refractive index increase Δn of two different sets of waveguides with increasing cross-sections, which were inscribed with different translation speeds and keeping all other inscription parameters the same. The waveguides were inscribed in the same substrate as the waveguides in Fig. 1(a) with pulse energy of 94 nJ using a 0.6 NA aspheric lens. The set inscribed with a sample translation speed of 4 mm/s presented higher maximum increase of the refractive index than the set inscribed with a speed of 8 mm/s which is attributed to the longer exposure time of the substrate at the focal region of the laser. Figure 1(c) shows the top view of a GLS waveguide with the line L1 along which the refractive index profile is measured.

As can be seen from Fig. 1(a) although the width of the waveguides is 4-6.6 μm the refractive index profiles present a small oscillation beyond the geometrical structure of the

waveguides, going below and then above the asymptotic bulk refractive index ($\Delta n = 0$), leading the total refractive index variation to extend up to $\sim 16 \mu\text{m}$. This variation beyond the area modified by the laser is attributed to residual stresses induced in the bulk by the ULI technique. The main mechanisms considered responsible for the refractive-index increase, observed in femtosecond-laser-written waveguides are densification [38] and stress [39] induced by the laser in the glass substrate. Therefore the area modified by the laser will inevitably impose a certain amount of stress to its adjacent regions even though unmodified by the laser, thus causing the refractive index variation to extend beyond the modified region.

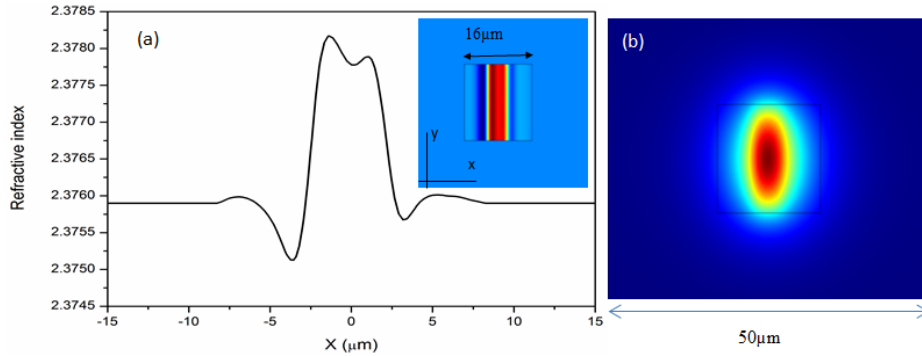


Fig. 2. (a) Measured refractive index profile along the x-axis of waveguide 3 imported in Comsol, inset shows the modelled x,y refractive index distribution at $1.55 \mu\text{m}$ (b) Calculated mode profile of the fundamental mode at $1.55 \mu\text{m}$ for the imported waveguide geometry generated with Comsol.

In order to better understand the waveguide confinement properties, we imported the measured x-axis refractive index profile of waveguide 3 presented in Fig. 1(a) into the commercially available Comsol Multiphysics software, as shown in Fig. 2(a). For the y-axis we assumed a uniform step-index structure. The inset shows the modelled x,y refractive index distribution at $1.55 \mu\text{m}$, where we used the refractive index of bulk GLS at $1.55 \mu\text{m}$ to be 2.3759. Figure 2(b) shows the calculated electric field profile of the fundamental mode at $1.55 \mu\text{m}$; this exhibited single mode operation. It is interesting to note that the obtained electric field profile is to a good approximation symmetric despite the asymmetric index distribution of the waveguide. This is due to the fact that at $1.55 \mu\text{m}$ the effective index of the fundamental mode is $n_{\text{eff}} \sim 2.3764$, which is well confined to the symmetric region of the waveguide. However, at shorter wavelengths, we could observe asymmetry in the electric field profile. The theoretical $1/e^2$ mode field diameters (MFDs) calculated by Comsol using the measured refractive index profile for waveguide 3 presented in Fig. 1(a) were $10.08 \mu\text{m}$ in the x-direction and $18 \mu\text{m}$ in the y-direction.

In order to verify the validity of the refractive index profiling the guiding properties of the waveguides were investigated by coupling $1.55 \mu\text{m}$ light into each waveguide and observing the mode profiles at the output facet. Figure 3(a) shows the end facet image of waveguide 3 from Fig. 1(a) when viewed under a microscope in transmission mode. Figure 3(b) shows the imaged output facet of the waveguide whilst coupling $1.55 \mu\text{m}$ light into it, exhibiting single mode guiding. The mode profile was imaged using a $40\times$ (0.65 NA) aspheric lens and captured using a Hamamatsu InGaAs infrared camera. The experimentally measured $1/e^2$ mode field diameters for the waveguide were found to be $10.98 \pm 1.15 \mu\text{m}$ in the x-axis and $17.68 \pm 2 \mu\text{m}$ in the y-axis in very good agreement with the theoretically simulated MFDs, thereby supporting the validity of the refractive index profiles. The waveguide mode cross-sections are shown in Fig. 3(c).

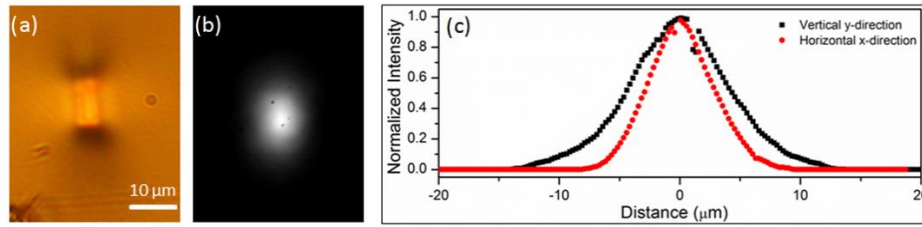


Fig. 3. (a) End facet image of waveguide 3 taken in transmission mode, (b) corresponding mode profile image for waveguide 3 pumped at 1.55 μm , and (c) the associated mode cross-sections at 1.55 μm in the vertical and horizontal directions.

4. Waveguide dispersion measurements

The material dispersion of the bulk substrate and the total dispersion of a series of inscribed waveguides was measured using white-light spectral-domain interferometry. The experimental setup for measuring the dispersion is shown in Fig. 4(a) and comprises a broadband mid-IR supercontinuum source ($\sim 1.3\text{-}4.5\ \mu\text{m}$), a balanced Mach-Zehnder free-space interferometer, and a scanning spectrometer ($0.4\text{-}5.0\ \mu\text{m}$).

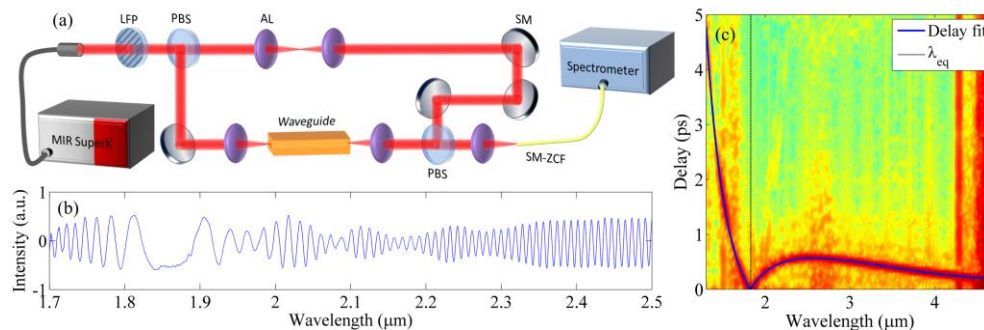


Fig. 4. (a) Experimental setup for measuring waveguide dispersion using a mid-IR supercontinuum source and a balanced Mach-Zehnder interferometer (LFP: Linear film polarizer, PBS: Plate beam splitter, AL: Aspheric lens, SM: Silver mirror, SM-ZCF: Single-mode ZBLAN collecting fiber). (b) Example interference spectrum with clearly resolved interference fringes. The gap at 1.85 μm marks the phase equalization wavelength (λ_{eq}) of the test and reference beams. (c) Short-time Fourier transform analysis of the interference spectrum displaying the differential delay of the test and reference beams, showing only a single guided mode.

Light was coupled to and collimated from the waveguides by aspheric lenses, and the two interfering beams were collected using a single-mode ZBLAN optical fiber. Proper guiding was verified by a PbSe focal plane array camera and optimized for maximum transmission by rotating the polarization of the source. Interference fringes, as seen in Fig. 4(b) were visible throughout the entire spectrum, providing around 600-700 interference extrema. These extrema were fitted to a fringe counting function using a modified Cauchy dispersion formula to model the wavelength dependence of the effective refractive index from which the dispersion was calculated [40]. From the interference spectrum, the guided mode properties of the waveguides were also investigated by short-time Fourier transform analysis. In Fig. 4(c) we show a spectrogram of the differential delay between the reference beam and the output of the largest tested waveguide ($\sim 12 \times 18\ \mu\text{m}$). The results clearly demonstrate that this waveguide is single-moded above 1.3 μm .

Figure 5(a) shows the measured dispersion of the bulk glass substrate compared to the dispersion of two waveguides with the same dimensions but fabricated using different NA

inscription lenses. For the waveguide inscribed with the 0.4 NA aspheric lens we used a pulse energy of 64 nJ and a sample translation speed of 12mm/s, while for the waveguide inscribed with the 0.6 NA aspheric lens we used a pulse energy of 110 nJ and a sample translation speed of 12mm/s. From Fig. 5(a) it is seen that the dispersion of the waveguides is very similar to that of the bulk glass, with negligible impact from changing the inscription parameters, such as, the NA of the inscription lens and the pulse energy.

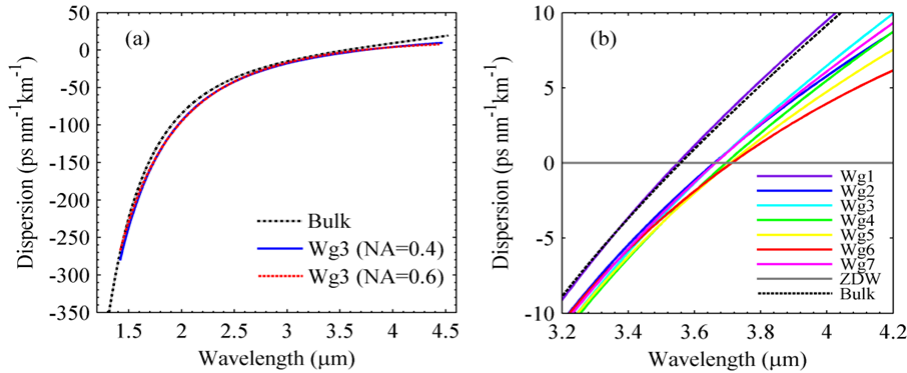


Fig. 5. (a) Comparison of the measured dispersion of the bulk glass and two waveguides of identical dimensions but fabricated using different focusing lens NA and different pulse energy. (b) Zoomed-in view of the dispersion around the ZDW of the bulk glass and seven waveguides inscribed with the same parameters but having increasing cross-sections with waveguide 1 having the smallest cross section and waveguide 7 having the largest one.

Figure 5(b) shows a zoomed-in view of the ZDW region of seven different waveguides, which all, except for waveguide 1, are seen to have almost identical dispersion curves. The waveguides were inscribed with a pulse energy of 110nJ and a sample translation speed of 12mm/s using a 0.6 NA aspheric lens, but they were chosen to have increasing widths with waveguide 1 being the narrowest and waveguide 7 being the widest. Waveguide 1 was measured to have a width of about 3 μm and every subsequent waveguide was 1.98 μm wider than the previous one so that the widest waveguide had a width of about 15 μm. The height was the same for all waveguides, about 18 μm. The bulk glass ZDW was identified to be around 3.61 μm, and for waveguide 1 the ZDW was at 3.55 μm, whereas the other six waveguides had a measured ZDW between 3.66 and 3.71 μm. The divergence of the dispersion curves at the long-wavelength edge of the spectrum is assumed to be primarily due to the limitations of the fit over a broad spectral range. The discrepancy regarding the ZDW between waveguide 1 and waveguides 2-7 is attributed to the fact that the index contrast of waveguide 1 is very weak so its dispersion should be very close to that of the bulk material.

In order to investigate the waveguide dispersion, the measured refractive index profiles of the waveguides were accurately imported into Comsol. The modelling revealed that the waveguide dispersion is indeed very small ($-1.77 \text{ ps nm}^{-1}\text{km}^{-1}$ at 2.5 μm); hence the total dispersion in the waveguides will be dominated by material dispersion, which is in agreement with the experimental observations.

5. Conclusion

We have used the ULI technique to fabricate waveguides embedded inside GLS substrates. The refractive index profiles of the waveguides were measured using QPM and the refractive index change due to the ULI was extracted along the horizontal axis. Valuable information regarding the effect the inscription parameters have on the refractive index profile was gained. Using the measured refractive index profiles the modal properties of the waveguides at 1.55 μm were modelled using the commercially available software Comsol. The simulated mode

field diameters of the waveguides were in excellent agreement with the experimentally measured MFDs when guiding 1.55 μm light in the waveguides, thereby supporting the validity of the measured refractive index profiles. The dispersion of the waveguides and the bulk GLS was measured over a broad range of wavelengths in the near and mid-IR region spanning from ~ 1.3 to $4.5 \mu\text{m}$. The ZDW for the waveguides and for the bulk substrate was determined to be between 3.66 and 3.71 μm for the waveguides and about 3.61 μm for the bulk. Furthermore the origin of the dispersion in the waveguides was investigated by importing the measured refractive index profiles into Comsol. The modelling revealed low waveguide dispersion, implying that the full dispersion in the waveguides will be dominated by material dispersion. Chalcogenide glasses due to their unique properties are a key technology for future telecommunications and mid-IR applications. The work done here helped obtain valuable information about ultrafast laser inscribed waveguides in GLS, a particularly appealing ChG glass, which open the potential for the realization of GLS ultrafast laser inscribed devices for telecommunications and mid-IR applications.

Acknowledgments

This work was funded in part through the EPSRC funded project ChAMP (EP/M015130/1), the Chalcogenide Advanced Manufacturing Partnership (<http://chalcogenide.net>). Heriot Watt University authors would like to acknowledge financial support from the UK Engineering and Physical Sciences Research Council (EPSRC, Grant number EP/G030227/1). The work of G Demetriou was supported by a James Watt scholarship from Heriot-Watt University. Technical University of Denmark authors acknowledge financial support from Innovation Fund Denmark for the projects Light & Food (J.No. 132-2012-3) and the project ShapeOCT (J. No. 4107-00011A), and from the European Commission through the Framework Seven (FP7) project MINERVA: MId- to NEaR infrared spectroscopy for improVed medical diAgnostics (317803; www.minerva-project.eu).